Ordering behavior of the two-dimensional Ising spin glass with long-range correlated disorder

L. Münster,[1] C. Norrenbrock,[1] A. K. Hartmann,[1,*] and A. P. Young[2]
[1]*Institut für Physik, Universität Oldenburg, 26111 Oldenburg, Germany*
[2]*University of California Santa Cruz, California 95064, USA*

(Received 1 February 2021; accepted 22 March 2021; published 12 April 2021)

The standard short-range two-dimensional Ising spin glass is numerically well accessible, in particular, because there are polynomial-time ground-state algorithms. On the other hand, in contrast to higher dimensional spin glasses, it does not exhibit a rich behavior, i.e., no ordered phase at finite temperature. Here, we investigate whether long-range correlated bonds change this behavior. This would still keep the model numerically well accessible while exhibiting a more interesting behavior. The bonds are drawn from a Gaussian distribution with a two-point correlation for bonds at distance r that decays as $(1 + r^2)^{-a/2}$, $a \geqslant 0$. We study numerically with exact algorithms the ground-state and domain-wall excitations. Our results indicate that the inclusion of bond correlations still does not lead to a spin-glass order at any finite temperature. A further analysis reveals that bond correlations have a strong effect at local length scales, inducing ferro- and antiferromagnetic domains into the system. The length scale of ferro- and antiferromagnetic order diverges exponentially as the correlation exponent approaches a critical value, $a \to a_{\text{crit}} = 0$. Thus, our results suggest that the system becomes a ferro- or antiferromagnet only in the limit $a \to 0$.

DOI: 10.1103/PhysRevE.103.042117

I. INTRODUCTION

Spin glasses are disordered magnetic materials which exhibit peculiar properties at very low temperatures [1]. To understand these materials, the Edwards-Anderson (EA) model and the Sherrington-Kirkpatrick (SK) model [2,3] have been developed. Spin glasses exhibit essential aspects of complex behavior [4] and research on spin glasses [5–7] has stimulated progress in numerous other fields, such as information processing [8], neuronal networks [9], discrete optimization [10,11], and Monte Carlo simulation [12].

In this paper, we study the two-dimensional EA spin-glass model with Ising spins. This model has short-range quenched random pairwise interactions, described in detail in Sec. II. Its properties are well described in the framework of the scaling and droplet picture [13–15], as has been confirmed by numerical calculations for large systems using exact ground state (GS) algorithms [16,17]. The model exhibits no finite-temperature spin-glass phase, in contrast to the three- or higher dimensional variants [18–20]. This is a bit unfortunate because spin glasses in higher dimensions are numerically much harder to treat compared to the two-dimensional short-range case. Thus, it is very desirable to find a two-dimensional variant, which exhibits a stable long-range ordered spin-glass phase. In this way, the numerical study of spin-glass ordering would become much simpler. It is the aim of the present paper to investigate a model variant, which carries the potential to induce long-range ordering.

At the zero-temperature phase transition, the behavior induced by the distribution of the interaction disorder, in particular, differences between continuous Gaussian and discrete bimodal $\pm J$ disorder distributions, have been the subject of intensive research [21–24]. Since the nonexistence of a finite-temperature spin-glass phase for short-range two-dimensional models is independent of the disorder distribution, here we consider only the Gaussian case. Previous works have shown how the increase of the mean of the Gaussian from zero to a sufficiently large value induces a ferromagnetic phase [25–29].

In this paper, we address how long-range correlations in the interactions (bonds) affect the ordering behavior. In particular, it is natural to believe that long-range correlations enhance the tendency of ordering. Thus, we want to investigate whether it leads to a low-temperature spin-glass phase for the two-dimensional system. Here, long range means that the bond correlation decays with a power law and so does not have a characteristic length scale. For disordered ferromagnets, the effects of long-range correlations have already been studied [30]. They found that if the exponent a of the power law is smaller than the dimension d of the system, the usual criterion for the relevance of quenched disorder with respect to the homogenous case is changed. Thus, with correlations falling off slowly enough, an effect on the presence of ordering may be visible.

Our paper was also partially motivated by a corresponding numerical study of the three-dimensional random-field Ising model with long-range correlation [31], where, for strong correlation, an influence on the quantitative ordering behavior has been observed for some critical exponents. Note, however, that the case of the random-field model is a bit different because the correlation acts on the random fields which provide local randomness competing against long-range ferromagnetic order. Consequently, from an extended Imry-Ma

*alexander.hartmann@uni-oldenburg.de

argument it was predicted [32] that the random-field Ising model with strong long-range correlation will show an increase of the lower critical dimension for ferromagnetic order. We note that there is no analogous prediction for the spin-glass case.

The following content is structured into three parts. First, the model is introduced and it is outlined how GS computations under changing boundary conditions (BCs) are used to produce domain wall (DW) excitations. Second, the results of the simulations will be presented. Finally, we give a discussion.

II. MODEL AND METHODS

A. The Ising spin glass with correlated bonds

The Ising spin glass consist of Ising spins $s_{\boldsymbol{m}} \in \{\pm 1\}$ on the sites $\boldsymbol{m} \in \Lambda$ of a two-dimensional lattice, i.e., $\Lambda \subset \mathbb{Z}^2$. In this paper, only square systems are considered, such that the spin glass has L spins in each direction and $|\Lambda| = L^2$. The Hamiltonian is given by

$$H_J(\boldsymbol{s}) = -\sum_{\{\boldsymbol{m},\boldsymbol{n}\}\in\mathcal{M}} J_{\boldsymbol{m},\boldsymbol{n}} s_{\boldsymbol{m}} s_{\boldsymbol{n}}\,, \tag{1}$$

where the sum runs over all pairs $\mathcal{M}$ of nearest-neighbor spin sites with periodic BCs in one and free BCs in the other direction. The bonds, $J_{\boldsymbol{m},\boldsymbol{n}}$, which represent the interaction between two spins, are random in strength and sign but remain constant over time. Hence, one speaks of a quenched disorder where the system is investigated under a fixed realization of the bonds, $\boldsymbol{J}$. Here, the bonds originate from a Gaussian random field, $J(\boldsymbol{x})$, which is a function of a *continuous* position $\boldsymbol{x}$, and has zero mean, $\langle J(\boldsymbol{x})\rangle = 0$ and a covariance given by

$$\langle J(\boldsymbol{x})J(\boldsymbol{x}+\boldsymbol{r})\rangle = (1+r^2)^{-a/2}, \tag{2}$$

$\boldsymbol{x}, \boldsymbol{r} \in \mathbb{R}^2$, $a \geqslant 0$ and $r = \|\boldsymbol{r}\|$. The entries of $\boldsymbol{J}$ are given by, $J_{\boldsymbol{m},\boldsymbol{n}} = J((\boldsymbol{m}+\boldsymbol{n})/2)$, which ensures that the correlation decays in the same manner along both axes. The correlation exponent, a, is the only parameter to control the correlation. For $a = 0$, one obtains the Ising model of a ferromagnet or antiferromagnet, respectively, depending on the bond realization. When $a \to \infty$, the uncorrelated Ising spin glass model with Gaussian disorder is recovered.

To generate the correlated bonds numerically, we utilized the Fourier filtering method (FFM) [31,33]. The FFM is a procedure to create stationary correlated random numbers of previously independent random numbers. Because it is based on the convolution theorem, it is possible to benefit from the computationally efficient fast Fourier transform algorithm [34]. For its implementation, we relied on the functions of the FFTW library, version 3.3.5 [35]. Figure 1 shows the average bond correlation along the main axes of a system with $|\Lambda| = 46^2$ spins calculated by the estimator:

$$C(\boldsymbol{r}) = \frac{1}{|\mathcal{M}'(\boldsymbol{r})|}\sum_{\{\boldsymbol{n},\boldsymbol{m}\}\in\mathcal{M}'(\boldsymbol{r})} \langle J_{\boldsymbol{m},\boldsymbol{n}} J_{\boldsymbol{m}+\boldsymbol{r},\boldsymbol{n}+\boldsymbol{r}}\rangle_J\,. \tag{3}$$

Here $\langle\ldots\rangle_J$ denotes the average with respect to the disorder. $\mathcal{M}'(\boldsymbol{r}) \subset \mathcal{M}$ contains those bonds $\{\boldsymbol{m},\boldsymbol{n}\}$ for which the bond $\{\boldsymbol{m}+\boldsymbol{r},\boldsymbol{n}+\boldsymbol{r}\}$ is also on the lattice. The fact that $\mathcal{M}'(\boldsymbol{r})$ does not contain all the bonds $\{\boldsymbol{n},\boldsymbol{m}\}$ in $\mathcal{M}$ is due to the free BCs in one direction. The point is that for vectors $\boldsymbol{r}$ which are not exactly parallel to the free boundary, the bond $\{\boldsymbol{m}+\boldsymbol{r},\boldsymbol{n}+\boldsymbol{r}\}$ does not exist for all bonds of $\mathcal{M}$. For the correlations shown in Fig. 1, we only investigated the directions parallel and perpendicular to the free boundary.

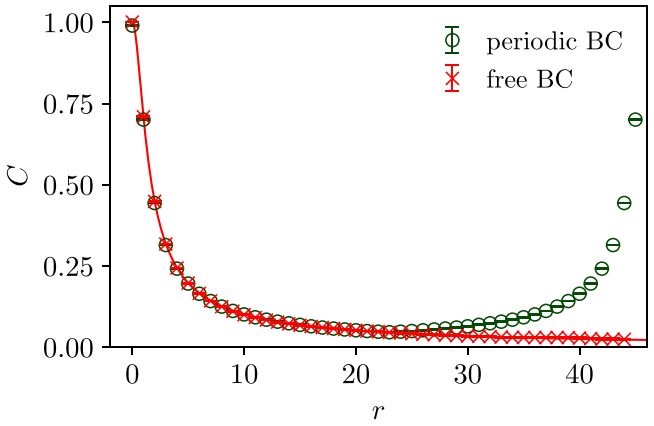

FIG. 1. Correlation of the bonds of a spin glass, calculated with Eq. (3), with $a = 1$ and $L = 46$ spins in each direction, x and y. The system has free boundary conditions in one direction and periodic boundary conditions in the other direction. The bond correlation was generated according to the Fourier filtering method (FFM) [31,33] with periodic boundary conditions in both directions, but the size in the directions of free boundaries was chosen much larger than the corresponding system size L. The line follows a fit of type $B_C(1+r^2)^{-A_C/2}$, yielding $B_C = 1.0003(12)$ and $A_C = 0.9953(13)$. The average was taken over 10 000 realizations of the disorder. The good agreement proves that the generation of the randomness works well.

B. Ground states and domain walls

The nature of the GS of the two-dimensional Ising spin glass is an intriguing subject on its own [36,37]. Furthermore, GS computations of finite systems are a well-established tool [10,11] to investigate the glassy behavior of the model in the zero-temperature limit [38]. The GS is the spin configuration which minimizes Eq. (1) for a given realization of the bonds. In the case of two-dimensional planar lattices, there exist exact procedures to generate the GS with a polynomial worst-case running time. This is in contrast to the three- or higher-dimensional variants which belong to the class of NP-hard problems [39]. Note that the planarity of the lattice allows for free BCs or for periodic BCs in one direction but not in both.

There is more than one approach to compute the GS of two-dimensional planar spin glasses, such as the algorithm of Bieche *et al.* [40] and that of Barahona *et al.* [41]. The key idea of these algorithms is to create a mapping from the original problem defined on the underlying lattice graph of the spin glass onto a related graph which is constructed in such a manner that the GS can be extracted from a *minimum-weight perfect matching*, which is polynomially computable. In this paper, we applied an ansatz which includes Kasteleyn city subgraphs into the mapping process and thus is more efficient [42,43] in terms of speed and memory usage than the above-mentioned algorithms. This allowed us to investigate systems

up to a linear system size of $L = 724$ spins in each direction without needing excessive computational resources. For the computation of the minimum-weight perfect matching, the Blossom *IV* algorithm [44] implemented by Rohe [45] was utilized.

To study whether an ordered spin-glass phase exists at nonzero temperature, it is actually not necessary to sample configurations at finite temperature. The basic idea is to create low-lying excitations for each realization by GS calculations of suitably modified variants of the realization. The excitations shall be extensive, i.e., destroy the long-range order. If the energy of these excitations typically grows with system size, this means an ordered phase is stable against thermal fluctuations [14]. On the other hand, if typical energies decrease with growing system sizes, arbitrary small energy fluctuations will be sufficient in equilibrium to destroy long-range order. Note that a growth of the typical energies can be observed either by having a distribution of excitation energies where the mean energy grows or where the mean value is zero but the variance, i.e., the width, grows. The former one corresponds to a ferromagnetic type of order, while the second one to spin-glass order.

Here, we create system-spanning DW excitations. This is done by computing GSs under periodic and antiperiodic BCs, also referred to as P-AP [46]. It works as follows. First, a spin glass with periodic BCs in one direction and free BCs in the other direction is generated with quenched disorder, $\boldsymbol{J}^{(\mathrm{p})}$. As mentioned above, the algorithm we used does not allow for fully periodic BCs, but having periodic BCs in one direction is sufficient. Then, its GS configuration, $\boldsymbol{s}^{(\mathrm{p})}_{\mathrm{gs}}$, is computed. Next, the periodic BCs are replaced by antiperiodic BCs by reversing the sign of one column of bonds parallel to the direction of periodicity, which leads to $\boldsymbol{J}^{(\mathrm{ap})}$. Afterward, the new GS configuration, $\boldsymbol{s}^{(\mathrm{ap})}_{\mathrm{gs}}$, is calculated. The change of the BCs imposes a DW of minimal energy between the two spin configurations $\boldsymbol{s}^{(\mathrm{p})}_{\mathrm{gs}}$ and $\boldsymbol{s}^{(\mathrm{ap})}_{\mathrm{gs}}$. The energy of the DW is given by

$$\Delta E = H_{\boldsymbol{J}^{(\mathrm{ap})}}\left(\boldsymbol{s}^{(\mathrm{ap})}_{\mathrm{gs}}\right) - H_{\boldsymbol{J}^{(\mathrm{p})}}\left(\boldsymbol{s}^{(\mathrm{p})}_{\mathrm{gs}}\right). \tag{4}$$

The geometrical structure of a DW can be characterized by the number $\mathcal{D}_L$ of bonds which are included in the surface. To avoid including those bonds which are a direct result of the different BCs, the surface is defined to consist of those bonds which fulfill $J^{(\mathrm{p})}_{\boldsymbol{m},\boldsymbol{n}} s^{(\mathrm{p})}_{\boldsymbol{m}} s^{(\mathrm{p})}_{\boldsymbol{n}} J^{(\mathrm{ap})}_{\boldsymbol{m},\boldsymbol{n}} s^{(\mathrm{ap})}_{\boldsymbol{m}} s^{(\mathrm{ap})}_{\boldsymbol{n}} < 0$, where $\boldsymbol{m}, \boldsymbol{n}$ runs over all unordered pairs of nearest-neighbor lattice sites [21].

III. RESULTS

We have obtained exact GSs for systems with correlation exponents in the range $a \in [10^{-3}, \infty]$, where $a = \infty$ corresponds to independently sampled bonds. Since the GS calculation requires only polynomial time as a function of the system size, we were able to study sizes up to a large value of $N \equiv L^2 = 724^2$ for each value of a. For each value of a and L, we performed an average over many realizations of the disorder, ranging from 10^6 realizations for the smallest sizes, 10 000 realizations for $L = 512$, to 2000 realizations for the largest system size.

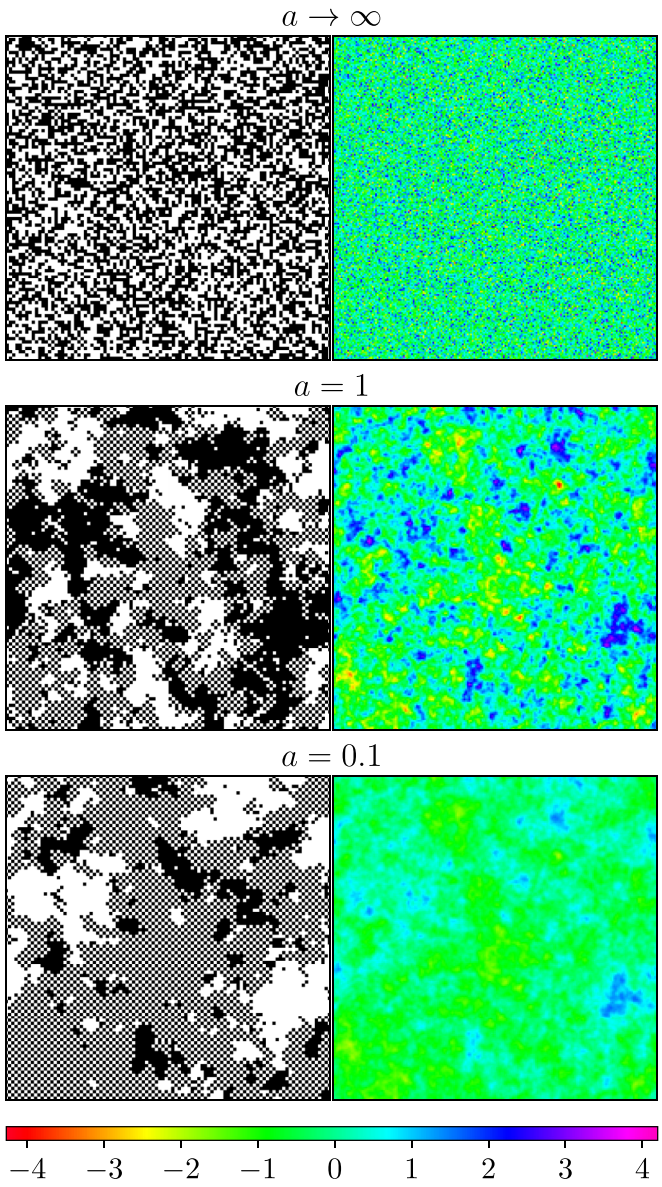

FIG. 2. The right-hand side of the figure shows one realization of the Gaussian random field. This is a function of continuous position but here we show it discretized with a spatial resolution of half a lattice spacing. From this continuous Gaussian random field, the bonds are extracted, at half lattice points. We show the Gaussian field for three different correlation exponents. The corresponding GSs are on the left. The correlations exponents are given by $a \to \infty$ (top), $a = 1$ (center), and $a = 0.1$ (bottom). Black points denote $s_{\boldsymbol{m}} = -1$ and white points $s_{\boldsymbol{m}} = 1$. In ferromagnetic order, two neighboring spins have same sign and in antiferromagnetic order the sign alternates. The system size is $L = 100$.

Figure 2 provides a first impression how the bond correlation impacts the ordering of the GS. It is apparent that, for strong correlations, there are large areas where the spins are either in ferromagnetic or antiferromagnetic order. This is related to there being large areas where, due to the correlation, the bonds have identical signs.

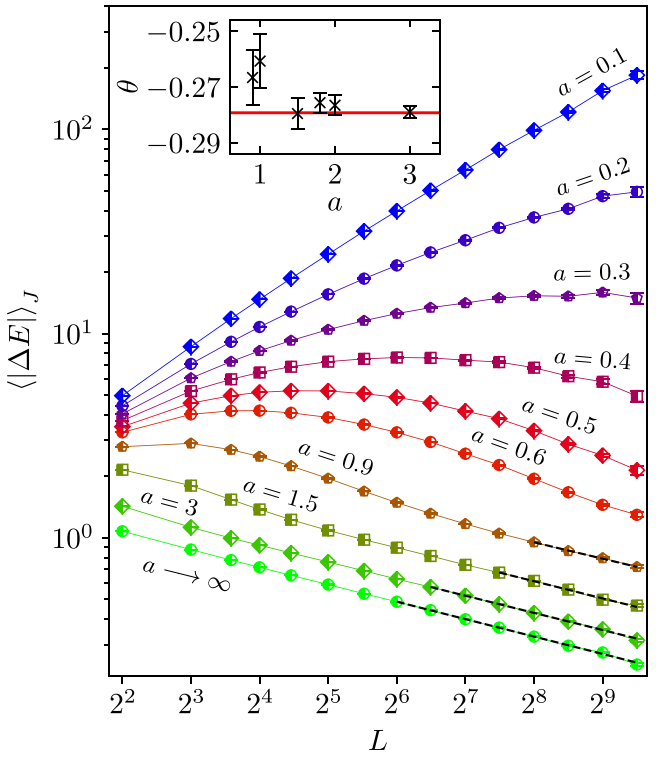

FIG. 3. Scaling of the average of the absolute value of the DW energy, $\langle|\Delta E|\rangle_J$, as a function of system size L for different values of a. The full lines are guides to the eyes only. The broken lines are fits of type $\langle|\Delta E|\rangle_J = A_\theta L^\theta$. The inset shows the values of θ which were obtained by fits for values of $a \geqslant 0.9$. The red line marks the value of the stiffness exponent for $a \to \infty$ according to Ref. [21].

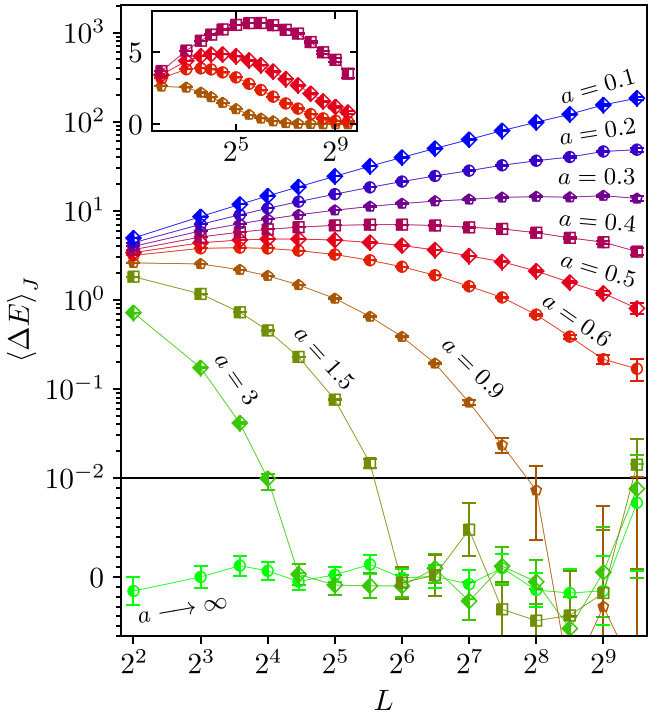

FIG. 4. A log-log plot of the average DW energy $\langle\Delta E\rangle_J$ as a function of the system size L for some values of correlation exponent a. The inset shows the same data with linear energy scale for $a = 0.4$, 0.5, 0.6, and 0.9 to highlight the peak structure. The lines are guides to the eyes only.

A. Domain-wall energy

Next, we look at the influence of bond correlation on the properties of the previously discussed DW excitations. The absolute value of the DW energy is proportional to the coupling strength between block spins in the zero-temperature limit [14]. A stable order is possible if the average absolute value of the DW energy increases with the system size. In the uncorrelated case, $a \to \infty$, one obtains a power-law behavior [14,20,21,47],

$$\langle|\Delta E|\rangle_J \sim L^\theta, \tag{5}$$

where θ is the stiffness exponent with its current best estimate $\theta = -0.2793(3)$ [21]. Since $\theta < 0$, there is no stable spin-glass phase for temperatures larger than zero. Figure 3 shows the impact of bond correlation on the scaling of $\langle|\Delta E|\rangle_J$. For $a \geqslant 0.9$, one can still observe the pure power-law decay of the uncorrelated model on sufficiently long length scales. The inset demonstrates that, in this region, the stiffness exponent stays constant at a value equal to that of the uncorrelated model. For values of $a \leqslant 0.9$, the average $\langle|\Delta E|\rangle_J$ initially grows with system size but starts to decrease for larger sizes, i.e., the curves exhibit a peak. The system size at the peak, L^*, shifts to larger system sizes on decreasing the correlation exponent a. This will be analyzed below.

First, we show in Fig. 4 the results for the average DW energy $\langle\Delta E\rangle_J$, which behaves in a somewhat similar manner as the average of the absolute value.

To understand our results better, we first consider a ferromagnet. The lowest-lying DW excitations are just straight lines, i.e., exhibit an energy $O(L)$ in a $L \times L$ system. Thus, with randomness, the DW energy distribution would exhibit an increasing mean as function of L, if order of ferromagnetic type existed. For true spin-glass order, there is no ferromagnetic order, hence, the mean would converge to zero. Furthermore, for a spin glass, say with a finite transition temperature $T_{\rm SG}$, the width of the bond distribution sets the scale of the transition temperature: If all bonds are multiplied by a factor of 2, corresponding to increasing the width of the distribution by a factor of two, $T_{\rm SG}$ will also be doubled. Conversely, a shrinking of the width corresponds to a decrease of $T_{\rm SG}$. Now, taking a renormalization point of view, note that the DW energy distribution corresponds to an effective distribution of bonds between block spins of size $b \equiv L$. Thus, if the width of the DW energy distribution shrinks, actually to zero, this means the effective $T_{\rm SG}$ will also shrink to zero when looking at larger and larger scales, i.e., there is no order at finite temperature. To summarize, if spin-glass order existed in this model for some value of a, one would observe an increase $\langle|\Delta E|\rangle_J$ in the limit $L \to \infty$, while at the same time $\langle\Delta E\rangle_J$ would remain at, or converge to, zero as a function of L. The latter indicates the absence of ferromagnetic order, but not necessarily the absence of spin glass order because for a spin glass the change of the BCs from periodic to antiperiodic is symmetric, i.e., could either increase or decrease the GS energy, so the average would be zero even in the case of spin glass order. An increase of both $\langle|\Delta E|\rangle_J$ and $\langle\Delta E\rangle_J$ for small

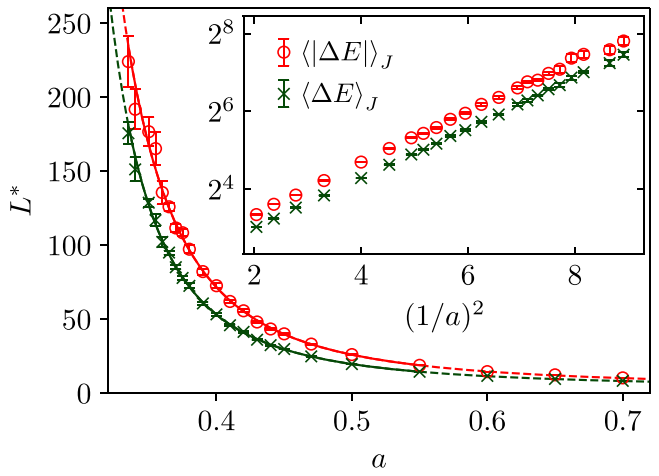

FIG. 5. The system size where the peak of $\langle|\Delta E|\rangle_J$ and $\langle\Delta E\rangle_J$ occurs, denoted by L^*, as a function of a. The lines are fits according to Eq. (6) in the range $a \leqslant 0.55$, see text for details. The broken lines are extrapolations of the fits. The inset shows L^* on a logarithmic scale as a function of $1/a^2$ exhibiting a straight-line behavior, and thus confirming the behavior obtained from the fit.

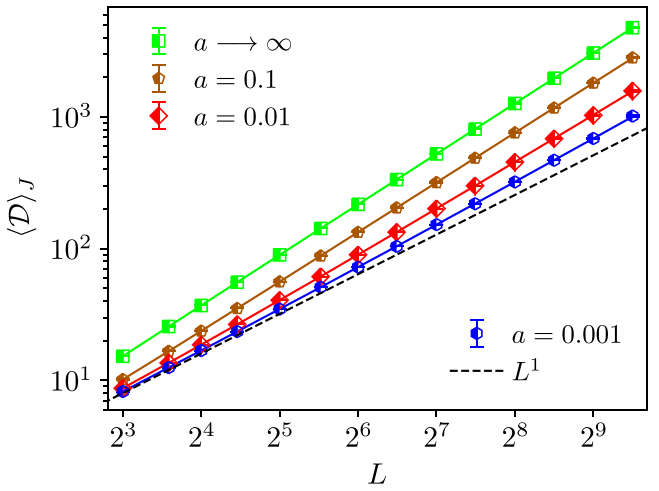

FIG. 6. Scaling of the DW surface area $\langle\mathcal{D}\rangle_J$ for different values of a. The broken black line shows the scaling of the DW surface in case of a ferro- and antiferromagnet. The full lines follow fits according to Eq. (8) with $L_{\min}^{(\mathrm{fit})} = 8$.

values of L and a corresponds to a ferro- and antiferromagnetic ordering on local length scales, which is visible in Fig. 2 and will be discussed more below. Whether there is a true ordered phase for very small values of a will be discussed next.

To track how the length scale of local order changes as a function of the correlation strength we measure the size at the peak, L^*, for both the DW energy and the absolute value, as a function of the correlation exponent a. Numerically, L^* was computed by fitting a parabola in the vicinity of the peaks of $\langle|\Delta E|\rangle_J$ and $\langle\Delta E\rangle_J$. As the fit in Fig. 5 demonstrates, the data for $L^*(a)$ is well described by an exponential function:

$$L^*(a) = A_L \exp\{b_L(a - a_{\mathrm{crit}})^{-c_L}\}. \tag{6}$$

A nonzero value of a_{crit} would indicate that an ordered phase exists for $a < a_{\mathrm{crit}}$. A true spin-glass phase would be possible if a_{crit} for $\langle\Delta E\rangle_J$ is smaller than a_{crit} for $\langle|\Delta E|\rangle_J$. We obtained values of $a_{\mathrm{crit}} = 0.13(0.10)$ for $\langle\Delta E\rangle_J$ and $0.10(0.17)$ for $\langle|\Delta E|\rangle_J$ with quality of the fit $Q = 0.87$ and $Q = 0.58$, respectively. Thus, a zero value for the critical correlation exponent parameter a_c seems likely.

To consider this further, we set a_{crit} to zero and obtain the values of the other fit parameters, which here are $A_L = 3.63(22)$, $b_L = 0.39(4)$, $c_L = 2.10(6)$ ($Q = 0.86$) for $\langle\Delta E\rangle_J$ and $A_L = 3.5(4)$, $b_L = 0.55(6)$, $c_L = 1.85(8)$ ($Q = 0.63$) for $\langle|\Delta E|\rangle_J$. Since the qualities of the fits remain almost identical in comparison to $a_{\mathrm{crit}} \neq 0$, the data is considered to be consistent with $a_{\mathrm{crit}} = 0$, which would imply that there is no global order when $a > 0$, either ferromagnetic or spin glass. The inset shows that the behavior of $L^*(a)$ is also compatible with $c_L = 2$. Fits of this type, with $a_{\mathrm{crit}} = 0$ and $c_L = 2$ fixed, have quality of the fit larger than 0.4, which is reasonable. Note that an exponential dependence of the breakup length scale of ferromagnetic order as a function of disorder strength was also found in the two-dimensional random field Ising model, both at low temperatures [48] and in the GS [49].

B. Domain wall surface

The behavior of DW surfaces is regarded as one of the essential parameters which describe the properties of random systems [50,51]. DWs separate spins in GSs and reversed GSs. Their surface is defined as those bonds which belong to the DW, and we denote the surface size by $\mathcal{D}$.

In the uncorrelated case, $a \to \infty$, the average DW surface size exhibits a power law [52,53],

$$\langle\mathcal{D}\rangle_J \sim L^{d_s}, \tag{7}$$

where d_s is the fractal surface dimension, for which the best numerical estimate at present is $d_s = 1.27319(9)$ [21]. When $a = 0$, the system is a ferro- or antiferromagnet and $\langle\mathcal{D}\rangle_J = L$, implying that $d_s = 1$, i.e., the surface is not fractal here. Figure 6 shows the scaling of the DW surface size for different values of a. In general, it can be seen that the correlation decreases the number of bonds in the DW surface. Even for $a = 0.001$, the data on this log-log plot shows a visible a visible deviation from the linear behavior which occurs for a strictly zero.

To characterize this behavior, we fitted pure power laws to the data. For this purpose, we did not do a full fit to all data points, but used the sliding-window approach instead. Here, four values of $\langle\mathcal{D}\rangle_J$ which are adjacent in terms of system size were grouped together in one fit window, respectively. The independent variables of such a fit window were given by (L_1, L_2, L_3, L_4) with $L_i < L_{i+1}$, $i = 1, ..., 4$. The dependent variables corresponded to the data, i.e., $\langle\mathcal{D}_{L_i}\rangle_J$. The smallest independent variable of each fit window is denoted as L_1.

For each window, we fitted the power law to the data resulting in a value of d_s. The dependence of d_s as a function of L_1 for different values of a can be found in Fig. 7. In the uncorrelated case, d_s decreases as a function of L_1, whereas for strong correlations d_s increases. In any case, for system sizes $L_1 < 32$ and small values $a \leqslant 1$, we observed some notable dependence of d_s on the system size. This motivated us to include corrections to scaling the power-law behavior in

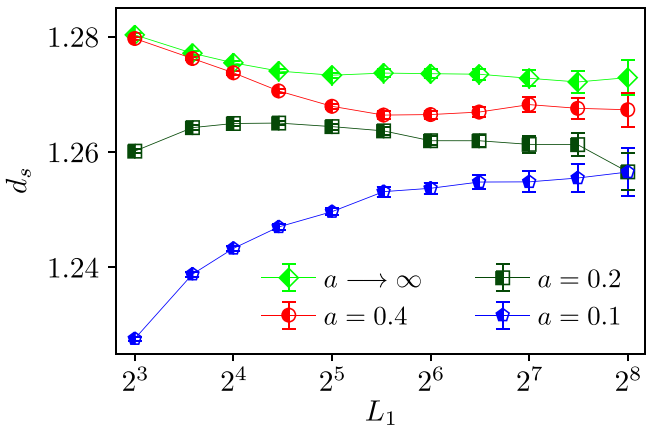

FIG. 7. The fractal surface dimension, d_s, of the DW surface area as a function of the smallest system size L_1 of a fit window.

Eq. (7) by considering [16,21]

$$\langle \mathcal{D} \rangle_J = A_{\mathcal{D}} L^{d_s} (1 + B_{\mathcal{D}} L^{-\omega_s}) . \tag{8}$$

By using Eq. (8), the quality of the fit is larger than 0.79 for all studied values of $a \leqslant 0.1$ with smallest linear system size of the fit $L_{\text{min}}^{(\text{fit})} = 8$. For larger values of a, the fit without correction term was always fine, given our statistical accuracy. Figure 8 shows the resulting fractal surface dimension for all considered values of a. At $a \approx 0.4$, the fractal surface dimension starts to decline from $d_s = 1.27319(9)$ [21], in the uncorrelated case, to smaller values. This is also visible in Fig. 7. Thus, it appears that for small values of a the fractal structure of the cluster changes, although there is no phase transition. Note that, to extract $d_s(a)$, we also performed fits of the form $d_s(L_1; a) = d_s(a) + \kappa_d L_1^{\gamma_d}$ (not shown; κ_d and γ_d also depend on a) to the sliding window fractal dimensions shown in Fig. 7. The behavior of this extrapolated fractal dimension also exhibits the same notable decrease of d_s for $a \leqslant 0.4$. Of course, it cannot be ruled out that on sufficiently large length scales, i.e., for much larger sizes than are currently accessible, the fractal dimension of the uncorrelated model would be

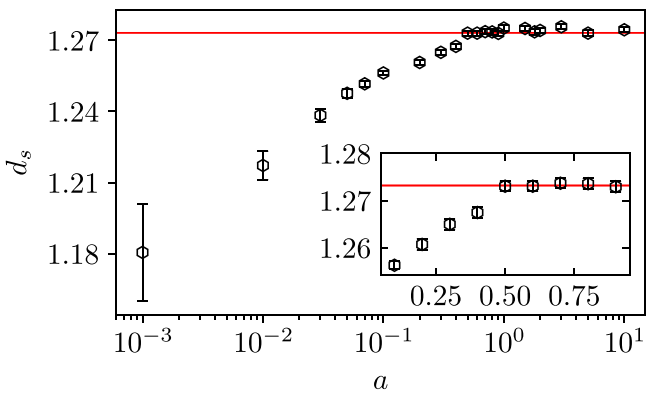

FIG. 8. The fractal surface dimension as a function of a. The values for $a \geqslant 0.2$ were obtained by pure power-law fits, i.e., $\langle \mathcal{D} \rangle_J = A_{\mathcal{D}} L^{d_s}$ with smallest system size used in the fits $L_{\text{min}}^{(\text{fit})} = 128$. The values for $a \leqslant 0.1$ were obtained from fits to Eq. (8), which includes the leading correction to scaling, with $L_{\text{min}}^{(\text{fit})} = 8$. The red line marks the value of d_s for $a \to \infty$ according to Ref. [21].

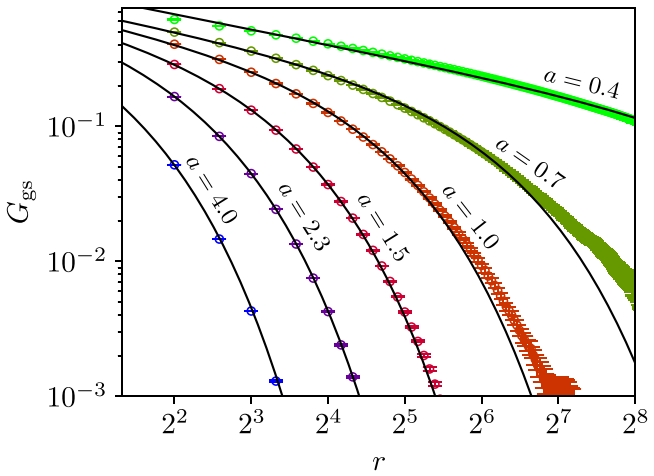

FIG. 9. Spin correlation of the GS for different values of a. The correlation was computed by utilizing the estimator of Eq. (9) along the main axes. The black lines are fits according to Eq. (10) when using a multifit, i.e., fitting two exponents υ and φ and many values of $\xi_{\text{gs}}(a)$ simultaneously to the correlation obtained for all values of a.

recovered again and thus $d_s = 1.27319(9)$ [21] for all values $a > 0$.

C. Spin correlations in the ground state

In this section, the effects of the bond correlations on spin correlations in the GS will be discussed. Note that at zero temperature there is no thermal disorder and, in our study which uses bonds with a continuous distribution, the GS is nondegenerate apart from overall spin inversion.

The two-point spin correlation is given by $\langle s_{\boldsymbol{m}}^{(\text{gs})} s_{\boldsymbol{m}+\boldsymbol{r}}^{(\text{gs})} \rangle_J$, where $s_{\boldsymbol{m}}^{(\text{gs})}$ denotes a spin in the GS configuration. In the uncorrelated model, $\langle s_{\boldsymbol{m}}^{(\text{gs})} s_{\boldsymbol{m}+\boldsymbol{r}}^{(\text{gs})} \rangle_J = 0$ if $\boldsymbol{r} \neq 0$. The correlated bonds induce a local ferro- and antiferromagnetic order into the GS. When $a = 0$, the system is a ferro- or antiferromagnet and the order is global. In the ferromagnetic case, $s_{\boldsymbol{m}}^{(\text{gs})} s_{\boldsymbol{m}+\boldsymbol{r}}^{(\text{gs})} = 1$ and in the antiferromagnetic case $s_{\boldsymbol{m}}^{(\text{gs})} s_{\boldsymbol{m}+\boldsymbol{r}}^{(\text{gs})}$ alternates between plus and minus one. Therefore, the GS spin correlation can be estimated by

$$G_{\text{gs}}(\boldsymbol{r}) = \frac{1}{|\Lambda'(\boldsymbol{r})|} \sum_{\boldsymbol{m} \in \Lambda'(\boldsymbol{r})} \left(\frac{\hat{\sigma}(\boldsymbol{r}) + 1}{2} \right) \left\langle s_{\boldsymbol{m}}^{(\text{gs})} s_{\boldsymbol{m}+\boldsymbol{r}}^{(\text{gs})} \right\rangle_J ,$$

$$\hat{\sigma}(\boldsymbol{r}) = \sigma(r_1)\sigma(r_2) \text{ with } \sigma(r_i) = \begin{cases} 1 & \text{if } r_i \text{ is even} \\ -1 & \text{if } r_i \text{ is uneven,} \end{cases} \tag{9}$$

and $\boldsymbol{r} = (r_1, r_2) \in \mathbb{Z}^2$. $\Lambda'(\boldsymbol{r}) \subset \Lambda$, similar to Eq. (3), contains those sites $\boldsymbol{m}$ for which $\boldsymbol{m} + \boldsymbol{r}$ is on the lattice, given the free BC in one direction. Note that this definition means that the correlation is measured for each site $\boldsymbol{m} \in \Lambda'$ on one of the two sublattices of a checkerboard partition of the square lattice, such that the correlation is insensitive to whether the order is ferromagnetic or antiferromagnetic.

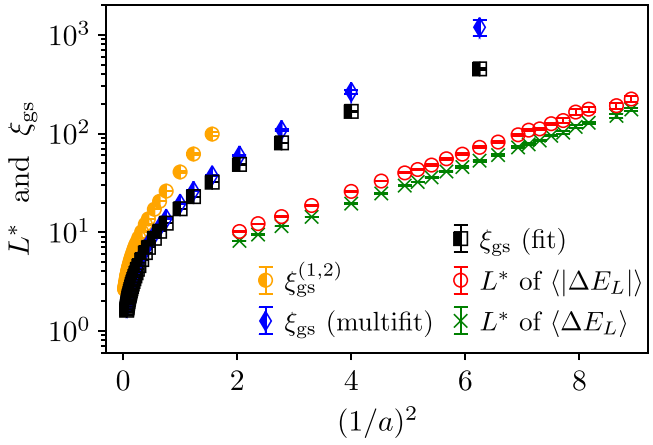

FIG. 10. The correlation length of the GS, $\xi_{gs}^{(1,2)}$, as a function of $1/a^2$, obtained by three different approaches. For comparison, the length scales $L^\star$ of the maxima are shown again.

In Fig. 9, one can see the GS correlation for different values of a. The data is well described by a scaling form of type

$$G_{gs}(r) \sim \frac{1}{r^\upsilon} \exp\left\{-\left(\frac{r}{\xi_{gs}}\right)^\varphi\right\}. \tag{10}$$

From the perspective of ordering, we are especially interested in the correlation length, ξ_{gs}, that provides the distance over which spins are notably correlated. The straightforward method to extract ξ_{gs} is by fitting the function of Eq. (10) to the data. The problem with such an approach is that neither υ nor φ are known. Also, finite-size corrections reduce the match between scaling form and actual data. Thus, we used different approaches to obtain ξ_{gs}.

First, we perform a separate *fit* for each value of a down to small correlations where the error bars start to exceed one quarter of the correlation value. We observed that for $a \geqslant 2$, the values of the exponents υ and φ did not change much, while for smaller values of a the exponents were a bit smaller. Therefore, we fixed the exponents to the (averaged) values seen for $a \geqslant 2$ and fitted only with respect to ξ_{gs}.

Second, we also performed a *multifit*, i.e., we fitted the correlation function simultaneously [54] with one value for υ, one value for φ and values of the correlation length at many values of a. The results of this multifit are also shown in Fig. 9. The obtained values for ξ_{gs} for these two fitting approaches are shown in Fig. 10. As can be seen, the results from fixing the values of the exponents and from using the multifit approach do not differ much.

Before we discuss the behavior of $\xi_{gs}(a)$, we describe the third approach we have used to estimate the correlation length. Here, we used the *integral estimator* that was introduced in Ref. [55]. It presupposes that for $r \leqslant \xi_{gs}$ the correlation function is dominated by a power law of type $r^{-\upsilon}$, whereas for $r > \xi_{gs}$ the correlation is negligible. As a consequence, the integral

$$I_k = \int_0^\infty \mathrm{d}r\, r^k G_{gs}(r) \tag{11}$$

is given by $I_k \propto (\xi_{gs})^{k+1-\upsilon}$ and thus

$$\xi_{gs}^{(k,k+1)} := \frac{I_{k+1}}{I_k} \propto \xi_{gs}\,. \tag{12}$$

This result would be exact and independent of k if the correlation actually was only a power law. For real correlations, the value of k dictates which part of the correlation function contributes most to the integral. Because such a scaling approach is only valid when r is much larger than the lattice constant a high value of k reduces the systematic error of the method. On the other hand, large values of k increase the statistical error of I_k. Following the recommendation of Ref. [56], we used $\xi_{gs}^{(1,2)}$ as a compromise. Note that since the statistical error of the measured correlation grows with distance r, one usually defines a cutoff distance up to which the data is directly used for the integral. Similar to Ref. [56], we specified this cutoff distance as the value of r where G_{gs} is smaller than three times its error. For values of r larger than this cutoff distance we computed the integral up to the maximal length of L from fits to Eq. (10). The start value of these fits were set to $r_{\min}^{(\mathrm{fit})} \geqslant 2$. Because it was observed that the correlation decays slightly differently along the directions with free and periodic BCs, the computations of the GS were also done with an independent set of simulations for full free BCs.

Next, the correlation length $\xi_{gs}^{(1,2)}$ was extracted from the average of the GS correlation, G_{gs}, along the main axes. The statistical error of $\xi_{gs}^{(1,2)}$ was estimated by bootstrapping [54,57] and the integrals according to Eq. (11) were computed by utilizing the midpoint integration rule. For small values of a, the contribution to I_k from the integral beyond the cutoff gets increasingly large. For instance, when $a = 1.15$ this contribution made up approximately 4% of the value of I_2. Hence, to estimate the total error, we added an extra systematic error to the statistical error. This was done by analyzing the value of $\xi_{gs}^{(1,2)}$ for two other choices of the cutoff distance, i.e., being the distance where the error of the correlation function is two or four times larger than its estimate, respectively. The maximal deviation of these two values from the standard definition, which uses a magnitude of three error bars to define cutoff, was set to be the systematic error. Furthermore, because the statistical error of I_k grows large for small values of the correlation exponent a and the system has to be sufficiently large to neglect boundary effects, values of $a < 0.8$ were not considered for this approach.

Figure 10 shows $\xi_{gs}^{(1,2)}$ as a function of the correlation exponent. In contrast to the data for the length scales $L^\star$, the plot shows that the behavior of none of the three correlation lengths that we have defined, ξ_{gs} (fit), ξ_{gs} (multifit) and $\xi_{gs}^{(1,2)}$, is close to exponential. Nonetheless, for $a \to 0$ the correlation lengths may converge to this behavior. We found that the data for these three definitions of the correlation length could be well fit to a function of the type

$$\xi_{gs} = A_\xi (a - a_{\mathrm{crit}})^{-d_\xi} \exp\{b_\xi (a - a_{\mathrm{crit}})^{-c_\xi}\}. \tag{13}$$

The exponential in Eq. (13) is consistent with the previous results for the length scale L^* and will dominate for $a \to 0$. The power-law part is chosen to describe the behavior for large values of a.

We have fitted the data to this function. For example, for the data obtained from the multifit, we again obtained a small value of $a_{\text{crit}} = 0.11(6)$. Thus, once again, we fixed $a_{\text{crit}} \equiv 0$ to determine the values of the remaining fit parameters, obtaining $A_\xi = 4.0(3)$, $d_\xi = 0.81(3)$, $b_\xi = 1.58(8)$, and $c_\xi = 1.19(4)$ with a good quality of the fit. Similar values, in particular for c_ξ, are found for the other two definitions of ξ_{gs} that we used. This means that for large values of the correlation exponent a the behavior of the correlation length as function of a seems to be better described by a power law. Also, the behavior of the peak lengths and of the ferromagnetic correlation lengths differ a lot, but it is still possible that for very small values of a, an exponential dependence of ξ_{gs} on $1/a^2$ would be recovered. Unfortunately, to investigate this issue, much larger system sizes would have to be treated, well beyond current numerical capabilities.

IV. DISCUSSION

The standard two-dimensional Ising spins glass does not exhibit a finite-temperature spin-glass phase in contrast to the three- or higher dimensional cases [18–20]. This work deals with the question how long-range correlated bonds influence this characteristic. Therefore, the ordering behavior of the two-dimensional Ising spin glass with spatially long-range correlated bonds is studied in the zero-temperature limit. The bonds are drawn from a standard normal distribution with a two-point correlation for bond distance r that decays as $(r^2+1)^{-a/2}$, $a \geqslant 0$. In the borderline case, when $a = 0$, the system is either a ferromagnet or antiferromagnet, depending on the bond realization. For $a \to \infty$, the uncorrelated EA model is recovered.

For $0 < a < \infty$, we observed that the correlation has local effects on the zero-temperature ordering behavior. The correlation locally effects the average value of the bonds as well as their standard deviation for each individual realization of the disorder. These parameters are decisive to distinguish between a spin glass or ferromagnet (antiferromagnet) in the case of the uncorrelated model [25,28]. In correspondence to that, the spin correlation of the GS reveals how the correlation induces a local ferro- or antiferromagnetic order into the GS. This is reflected by a growing correlation length $\xi_{\text{gs}}(a)$ when decreasing a.

Complementary results to the direct study of the GS spin configurations were obtained by investigating DW excitations. The average of the absolute value of the DW energy can be interpreted as the coupling strength between block spins at zero temperature [14]. We found that for strong bond correlations, the average of absolute value of the DW energy initially increases as a function of the system size up to a peak and then decreases. Since we made the same observation for the actual DW energy, it shows that the increase of the absolute value of the DW energy is a consequence of local ferro- or antiferromagnetic order of the system in GS. The system size where the peak occurs, L^*, is interpreted as the length scale of local order. For small values of the correlation exponent a, both $L^*(a)$ and the correlation length of the GS, $\xi_{\text{gs}}(a)$, can be described by an exponential divergence. Interestingly, a similar exponential length scale was also found in the two-dimensional random field Ising model by GS computations [49] and at low temperatures [48]. In these studies, the length scale of ferromagnetic order was examined as a function of the standard deviation of the random magnetic field.

For the two-dimensional Ising spin glass, the distribution of the absolute value of the DW energy is universal with respect to the initial bond distribution. This means for any continuous, symmetric bond distribution with sufficiently small mean and finite higher moments, the absolute value of the DW energy should approach the same scaling function [13,14,58]. Thus, we expect the same kind of universality for our model.

The stiffness exponent θ describes the scaling of the width of this distribution and is related to the critical exponent ν describing the divergence of the correlation length as $T \to 0$ by $\nu = -1/\theta$ [14,24]. At this zero temperature transition, ν is the only independent exponent. Therefore, any bond correlation which leaves the stiffness exponent unchanged does not influence the universality of the model. From the data of L^*, it is expected that there is no global ordered phase for $a > 0$. This implies that the stiffness exponent is negative for $a > 0$. Furthermore, for values of a in the range $a \geqslant 0.9$ the stiffness exponent stays equal to the uncorrelated case. Due to the limited range of studied length scales, it was not possible for us to verify this for values of a less than 0.9.

In addition to the DW energy, another important parameter to describe the low-temperature behavior of the Ising spin glass is the DW surface area [50,51]. In the uncorrelated model, the DW surface area follows a power law, $\langle \mathcal{D} \rangle_J \sim L^{d_s}$, where $d_s = 1.27319(9)$ [21]. Our results are compatible to this for all considered correlation exponents $a \geqslant 0.5$. At $a \approx 0.4$ the fractal surface dimension starts to decline. For the values of $a \leqslant 0.1$ the data is well described by a power law with scaling corrections [16,21], i.e., $\langle \mathcal{D} \rangle_J = A_{\mathcal{D}} L^{d_s}(1 + B_{\mathcal{D}} L^{-\omega_s})$. The decrease in d_s implies that, for strong correlations, DWs with shorter lengths are energetic favorable. In the extreme case when $a = 0$, the system is a ferro- or antiferromagnet and thus $d_s = 1$. Of course, it cannot be ruled out that the decline in d_s is local and on sufficiently long length scales the pure power law with $d_s = 1.27319(9)$ [21] is recovered again for all $a > 0$.

In this context, it is interesting to note that there exists a proposed relation which links the stiffness exponent with the fractal surface dimension, namely, $d_s = 1 + 3/[4(3+\theta)]$ [59]. According to highly accurate numerical results [21], this equation is probably not exact. Our results for the fractal surface dimension $d_s = 1.27318(29)$ ($Q = 0.99$) and the stiffness exponent $\theta = -0.2815(13)$ ($Q = 0.13$) deviate by approximately 6.5 standard deviations from the mentioned conjecture, since $d_s - 1 - 3/[4(3+\theta)] = -0.0027(4)$. The latter result was obtained by using standard error propagation, thus neglecting correlations between the estimates of d_s and θ which exist because both values were obtained from the same data set. Nonetheless, our results also support the conclusion that the proposed scaling relation is not exact.

In conclusion, it is observed that correlation among the bonds has a strong effect on the ordering on local length scales, inducing ferro- and antiferromagnetic domains into the GS. The length scale of local ferro- and antiferromagnetic order diverges exponentially when the correlation exponent approaches zero. The fractal surface dimension decreases for strong correlations on the studied length scales. No signature of a spin-glass phase at finite temperature is observed.

ACKNOWLEDGMENTS

A.P.Y. thanks the Alexander von Humboldt Foundation for financial support through a Research Award. The simulations were performed at the HPC cluster CARL, located at the University of Oldenburg (Germany) and funded by the DFG through its Major Research Instrumentation Programme (INST 184/157-1 FUGG) and the Ministry of Science and Culture (MWK) of the Lower Saxony State.

[1] E. Vincent and V. Dupuis, in *Frustrated Materials and Ferroic Glasses*, edited by T. Lookman and X. Ren (Springer, Cham, 2018), pp. 31–56.
[2] S. F. Edwards and P. W. Anderson, J. Phys. F **5**, 965 (1975).
[3] D. Sherrington and S. Kirkpatrick, Phys. Rev. Lett. **35**, 1792 (1975).
[4] D. L. Stein and C. M. Newman, *Spin Glasses and Complexity* (Princeton University Press, Princeton, 2013).
[5] M. Mézard, G. Parisi, and M. Virasoro, *Spin Glass Theory and Beyond* (World Scientific, Singapore, 1987).
[6] *Spin Glasses and Random Fields*, edited by A. P. Young (World Scientific, Singapore, 1998).
[7] *Spin Glasses*, edited by E. Bolthausen and A. Bovier (Springer, Berlin, 2007).
[8] H. Nishimori, *Statistical Physics of Spin Glasses and Information Processing: An Introduction* (Oxford University Press, Oxford, 2001).
[9] V. Dotsenko, *An Introduction to the Theory of Spin Glasses and Neural Networks* (World Scientific, Singapore, 1994).
[10] A. K. Hartmann and H. Rieger, *Optimization Algorithms in Physics* (Wiley-VCH, Weinheim, 2002).
[11] *New Optimization Algorithms in Physics*, edited by A. K. Hartmann and H. Rieger (Wiley-VCH, Weinheim, 2004).
[12] Z. Zhu, A. J. Ochoa, and H. G. Katzgraber, Phys. Rev. Lett. **115**, 077201 (2015).
[13] W. L. McMillan, J. Phys. C **17**, 3179 (1984).
[14] A. J. Bray and M. A. Moore, in *Heidelberg Colloquium on Glassy Dynamics*, edited by J. van Hemmen and I. Morgenstern (Springer, Berlin, 1987), pp. 121–153.
[15] D. S. Fisher and D. A. Huse, Phys. Rev. B **38**, 386 (1988).
[16] A. K. Hartmann and M. A. Moore, Phys. Rev. Lett. **90**, 127201 (2003).
[17] A. K. Hartmann and M. A. Moore, Phys. Rev. B **69**, 104409 (2004).
[18] A. P. Young and R. B. Stinchcombe, J. Phys. C **9**, 4419 (1976).
[19] B. W. Southern and A. P. Young, J. Phys. C **10**, 2179 (1977).
[20] A. K. Hartmann and A. P. Young, Phys. Rev. B **64**, 180404(R) (2001).
[21] H. Khoshbakht and M. Weigel, Phys. Rev. B **97**, 064410 (2018).
[22] F. Parisen Toldin, A. Pelissetto, and E. Vicari, Phys. Rev. E **84**, 051116 (2011).
[23] C. K. Thomas, D. A. Huse, and A. A. Middleton, Phys. Rev. Lett. **107**, 047203 (2011).
[24] L. A. Fernandez, E. Marinari, V. Martin-Mayor, G. Parisi, and J. J. Ruiz-Lorenzo, Phys. Rev. B **94**, 024402 (2016).
[25] D. Sherrington and W. Southern, J. Phys. F **5**, L49 (1975).
[26] C. Amoruso and A. K. Hartmann, Phys. Rev. B **70**, 134425 (2004).
[27] R. Fisch and A. K. Hartmann, Phys. Rev. B **75**, 174415 (2007).
[28] C. Monthus and T. Garel, Phys. Rev. B **89**, 184408 (2014).
[29] H. Fajen, A. K. Hartmann, and A. P. Young, Phys. Rev. E **102**, 012131 (2020).
[30] A. Weinrib and B. I. Halperin, Phys. Rev. B **27**, 413 (1983).
[31] B. Ahrens and A. K. Hartmann, Phys. Rev. B **84**, 144202 (2011).
[32] T. Nattermann, in *Spin Glasses and Random Fields*, edited by A. P. Young (World Scientific, Singapore, 1998), pp. 277–298.
[33] H. A. Makse, S. Havlin, M. Schwartz, and H. E. Stanley, Phys. Rev. E **53**, 5445 (1996).
[34] J. W. Cooley and J. W. Tukey, Math. Comput. **19**, 297 (1965).
[35] M. Frigo and S. G. Johnson, Proc. IEEE **93**, 216 (2005).
[36] C. M. Newman and D. L. Stein, Phys. Rev. Lett. **84**, 3966 (2000).
[37] L.-P. Arguin and M. Damron, Ann. Inst. Henri Poincare **50**, 28 (2014).
[38] A. K. Hartmann, in *Rugged Free Energy Landscapes*, edited by W. Janke (Springer, Berlin, 2008), pp. 67–106.
[39] F. Barahona, J. Phys. A **15**, 3241 (1982).
[40] L. Bieche, J. P. Uhry, R. Maynard, and R. Rammal, J. Phys. A **13**, 2553 (1980).
[41] F. Barahona, R. Maynard, R. Rammal, and J. Uhry, J. Phys. A **15**, 673 (1982).
[42] G. Pardella and F. Liers, Phys. Rev. E **78**, 056705 (2008).
[43] C. K. Thomas and A. A. Middleton, Phys. Rev. B **76**, 220406(R) (2007).
[44] W. Cook and A. Rohe, INFORMS J. Comput. **11**, 138 (1999).
[45] A. Rohe, The Blossom Four Code for Min-Weight Perfect Matching, https://www.math.uwaterloo.ca/~bico/blossom4/.
[46] A. C. Carter, A. J. Bray, and M. A. Moore, Phys. Rev. Lett. **88**, 077201 (2002).
[47] A. K. Hartmann, A. J. Bray, A. C. Carter, M. A. Moore, and A. P. Young, Phys. Rev. B **66**, 224401 (2002).
[48] E. Pytte and J. F. Fernandez, J. Appl. Phys. **57**, 3274 (1985).
[49] E. T. Seppälä, V. Petäjä, and M. J. Alava, Phys. Rev. E **58**, R5217 (1998).
[50] A. J. Bray and M. A. Moore, Phys. Rev. Lett. **58**, 57 (1987).
[51] C. M. Newman and D. L. Stein, in *Spin glasses*, edited by E. Bolthausen and A. Bovier (Springer, Berlin, 2007), pp. 145–158.
[52] N. Kawashima, J. Phys. Soc. Jpn. **69**, 987 (2000).

[53] O. Melchert and A. K. Hartmann, Phys. Rev. B **76**, 174411 (2007).

[54] A. K. Hartmann, *Big Practical Guide to Computer Simulations* (World Scientific, Singapore, 2015).

[55] F. Belletti, M. Cotallo, A. Cruz, L. A. Fernandez, A. Gordillo-Guerrero, M. Guidetti, A. Maiorano, F. Mantovani, E. Marinari, V. Martin-Mayor, A. M. Sudupe, D. Navarro, G. Parisi, S. Perez-Gaviro, J. J. Ruiz-Lorenzo, S. F. Schifano, D. Sciretti, A. Tarancon, R. Tripiccione, J. L. Velasco, and D. Yllanes, Phys. Rev. Lett. **101**, 157201 (2008).

[56] F. Belletti, A. Cruz, L. A. Fernandez, A. Gordillo-Guerrero, M. Guidetti, A. Maiorano, F. Mantovani, E. Marinari, V. Martin-Mayor, J. Monforte, *et al.*, J. Stat. Phys. **135**, 1121 (2009).

[57] A. P. Young, *Everything You Wanted to Know About Data Analysis and Fitting but Were Afraid to Ask* (Springer, Cham, 2015).

[58] C. Amoruso, E. Marinari, O. C. Martin, and A. Pagnani, Phys. Rev. Lett. **91**, 087201 (2003).

[59] C. Amoruso, A. K. Hartmann, M. B. Hastings, and M. A. Moore, Phys. Rev. Lett. **97**, 267202 (2006).